

REGULARIZATION OF THE HILL FOUR-BODY PROBLEM WITH OBLATE BODIES

EDWARD BELBRUNO, MARIAN GIDEA, AND WAI-TING LAM

ABSTRACT. We consider the Hill four-body problem where three oblate, massive bodies form a relative equilibrium triangular configuration, and the fourth, infinitesimal body orbits in a neighborhood of the smallest of the three massive bodies. We regularize collisions between the infinitesimal body and the smallest massive body, via McGehee coordinate transformation. We describe the corresponding collision manifold and show that it undergoes a bifurcation when the oblateness coefficient of the small massive body passes through the zero value.

1. INTRODUCTION

We consider the Hill approximation of the circular restricted four-body problem with oblate bodies, on the motion of an infinitesimal body under the gravitational influence of three massive bodies of oblate shapes; the three bodies are assumed to be in a relative equilibrium triangular configuration, and the motion of the infinitesimal body is assumed to take place in a neighborhood of the smallest of the three bodies, which we think of as an asteroid. See [BGCG⁺20]. The resulting gravitational field in the Hill approximation contains a non-Newtonian term which depends on the oblateness coefficient of the asteroid. We use McGehee coordinates to regularize collisions between the infinitesimal body and the asteroid, which amounts to blowing up the collision set to a manifold that captures the dynamics in the singular limit. (Note that, due to the non-Newtonian term in the potential, the Levi-Civita regularization does not apply to this setting.) We describe the collision manifold and the regularized dynamics in a neighborhood of it. We show that each collision solution is branch regularizable, and each extension of a collision solution is a reflection. We also show that the collision manifold is not block regularizable. Moreover, we show that the collision manifold undergoes a double saddle-node bifurcation as the oblateness coefficient of the asteroid passes through the zero value. When the shape of the asteroid becomes prolate, no collisions between the infinitesimal body and the asteroid are possible.

The four body system that we consider here can be viewed as a model for the Sun-Jupiter-Hektor-Skamandrios system; Hektor is a Jupiter's trojan

E.B. and M.G. were partially supported by NSF grant DMS-1814543.

W-T.L. was partially supported by NSF grant DMS-1814543 and DMS-2138090.

asteroid, and Skamandrios is a moonlet of Hektor. Hektor’s shape can be approximated by a dumb-bell figure and has one of the largest oblateness coefficients amongst objects of similar size in the solar system [Des15]. The moonlet Skamandrios appears to have a complicated orbit, which is close to 1:10 and 2:21 orbit/spin resonances; a small change could potentially eject the moonlet or make it collide with the asteroid [MDCR⁺14]. This justifies our interest in understanding collision orbits.

McGehee coordinate transformation was introduced in [McG81] to regularize collisions in a central force field of the form $U(\mathbf{x}) = |\mathbf{x}|^{-\alpha}$, where $\mathbf{x} \in \mathbb{R}^2$ and $\alpha > 0$. He also introduced the concept of branch regularization. A solution is branch regularizable if it has a unique real analytic extension past the collision. Branch regularization concerns the extension of individual solutions. The concept of block regularization considers collective extensions of solutions; it was introduced by Easton in [Eas71] who referred to it as ‘regularization by surgery’. A flow is called block regularizable if it is diffeomorphic to the trivial parallel flow in a deleted neighborhood of the collision set.

McGehee transformation has been applied to show the existence of ejection-collision orbits, which start and end at a collision. Llibre showed analytically the existence of ejection-collision orbits in the restricted three-body problem [Lli82], Lacomba and Llibre showed numerically the existence of transverse ejection-collision orbits in the Hill problem for some value of the energy [LL88], while Delgado-Fernández showed analytically the existence of such orbits for all sufficiently small energies in [Fer88]. Other related works include [Dev81, Pin95, ORS18, ARBMO21].

McGehee regularization can also be applied to quasi-homogeneous central force fields of the form $U(\mathbf{x}) = \gamma_1|\mathbf{x}|^{-\alpha_1} + \gamma_2|\mathbf{x}|^{-\alpha_2}$, with $\gamma_1, \gamma_2, \alpha_1, \alpha_2 > 0$; see [SSM00]. Belbruno used McGehee transformation to regularize collisions with a black hole in [BP11] in order to establish the relationship between the null geodesic structure of the Schwarzschild black hole solution, and the corresponding inverse-cubic Newtonian central force problem. Belbruno and collaborators also used the McGehee transformation to study the regularizability of the big bang singularity, including the case when random perturbations modeled by Brownian motion are present in the system [Bel13, XB14, BX18]. Other applications of related interest include [DMS00, GM14, EIB09, ORS22].

A contribution of our work is that we perform McGehee regularization of collisions in a four-body problem (rather than in a central force field), where the non-Newtonian part of the gravitational potential is owed to the shape of the body. As a matter of fact, our work assumes a more general setting, of a Hill four-body problem with a general quasi-homogenous potential, which includes the oblateness effect as a particular case. Another contribution is that we perform a bifurcation analysis as the oblateness coefficient varies, with the surprising conclusion that collisions cease to occur as we switch from oblate to prolate shape.

2. SETUP AND MAIN RESULT

2.1. Hill four-body problem with oblate bodies. In this section we describe the Hill approximation of the circular restricted four-body problem with oblate massive bodies. This problem concerns the dynamics of an infinitesimal body (particle) moving in a plane under the gravitational influence of three oblate bodies of masses $m_1 > m_2 > m_3$, but without influencing their motion. We refer to these three bodies as primary, secondary, and tertiary, respectively. We express the gravitational potential of each body in terms of spherical harmonics truncated up to second order zonal harmonic, that is,

$$(2.1) \quad V_i(x_1, x_2, x_3) = \frac{m_i}{r} + \frac{m_i}{r} \left(\frac{R_i}{r} \right)^2 \left(\frac{C_{20}^i}{2} \right) \left(3 \left(\frac{x_3}{r} \right)^2 - 1 \right)$$

where $r = (x_1^2 + x_2^2 + x_3^2)^{1/2}$, R_i is the average radius of the i -th body, and the gravitational constant is normalized to 1. The dimensionless quantity C_{20}^i is the coefficient of the zonal harmonic of order 2, with $C_{20}^i < 0$ for an oblate body, $C_{20}^i = 0$ for a spherical body, and $C_{20}^i > 0$ for a prolate body. Further, we denote $C_i = C_{20}^i R_i^2 / 2$.

For the circular restricted four-body problem, the assumption is that the three massive bodies are in a relative equilibrium configuration, that is, they move on circular orbits around their center of mass while preserving their mutual distances constant over time. In the case when the bodies have no oblateness, the only non-collinear relative equilibrium configuration is the Lagrangian equilateral triangle. When the bodies are oblate, the gravitational potential is no longer Newtonian, and the relative equilibrium is no longer an equilateral triangle. It has been shown in [BGCG⁺20] that there is a unique relative equilibrium which is a scalene triangle. Such triangle has the property that the body with the larger C_i is opposite to the longer side of the triangle. We normalize the units of distance so that the distance between m_1 and m_2 is set to 1, and we let u_1 be the distance from m_1 to m_3 , and u_2 be the distance from m_2 to m_3 . See Fig. 2.1. The sides u_1 and u_2 are uniquely determined by the implicit equations

$$(2.2) \quad 1 - 3C_{12} = \frac{1}{u_1^3} - \frac{3C_{13}}{u_1^5} = \frac{1}{u_2^3} - \frac{3C_{23}}{u_2^5},$$

where we denote $C_{ij} = C_i + C_j$.

Given such a relative equilibrium configuration, the motion of the particle in a vicinity of the tertiary is described by the Hamiltonian of the circular restricted four-body problem (see, e.g., [BGCG⁺20]). However, the corresponding Hamiltonian equations are difficult to treat analytically. Therefore we consider below the Hill approximation of the circular restricted four-body problem. This is derived by rescaling the distances by a factor of $m_3^{1/3}$, writing the associated Hamiltonian in the rescaled coordinates as a power

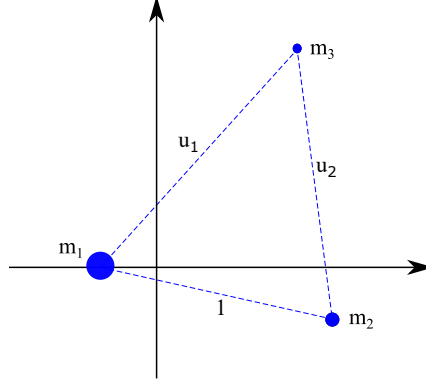


FIGURE 1. Scalene triangle relative equilibrium.

series in $m_3^{1/3}$, and neglecting all the terms of order $O(m_3^{1/3})$ in the expansion. The oblateness coefficient C_i also gets rescaled to $c_i = m_3^{-2/3} C_{20}^i R_i^2 / 2$. This procedure yields an approximation of the motion of the particle in an $O(m_3^{1/3})$ -neighborhood of the tertiary, while the primary and the secondary are ‘sent to infinity’. We obtain a much simpler Hamiltonian than the one for the circular restricted four-body problem, for which the contribution of the primary and of the secondary to the gravitational potential is given by a quadratic polynomial. Specifically, the Hamiltonian of the Hill four-body problem relative to some convenient co-rotating frame is given by

(2.3)

$$\begin{aligned}
 H = & \frac{1}{2}(y_1^2 + y_2^2 + y_3^2) + x_2 y_1 - x_1 y_2 \\
 & + \left(\frac{1 - \lambda_2}{2}\right) x_1^2 + \left(\frac{1 - \lambda_1}{2}\right) x_2^2 + \frac{1}{2} \left(\frac{(1 - \mu)}{u_1^3} + \frac{\mu}{u_2^3}\right) x_3^2 \\
 & - \left(\frac{(1 - \mu)c_1}{u_1^3}\right) \left(3 \left(\frac{x_3}{u_1}\right)^2 - 1\right) - \left(\frac{\mu c_2}{u_2^3}\right) \left(3 \left(\frac{x_3}{u_2}\right)^2 - 1\right) \\
 & - \frac{1}{(x_1^2 + x_2^2 + x_3^2)^{1/2}} - \frac{c_3}{(x_1^2 + x_2^2 + x_3^2)^{3/2}} \left(\frac{3x_3^2}{x_1^2 + x_2^2 + x_3^2} - 1\right).
 \end{aligned}$$

where $\mu = \frac{m_2}{m_1 + m_2}$, and λ_1 and λ_2 are given by the following formulas

$$\begin{aligned}
 \lambda_1 = & \frac{1}{2} \left(2 - \frac{2(1 - \mu)}{u_1^5} - \frac{2\mu}{u_2^5} + \frac{3(1 - \mu)}{u_1^3} + \frac{3\mu}{u_2^3} - \frac{3}{u_1^3 u_2^3} \sqrt{\Delta} \right), \\
 \lambda_2 = & \frac{1}{2} \left(2 - \frac{2(1 - \mu)}{u_1^5} - \frac{2\mu}{u_2^5} + \frac{3(1 - \mu)}{u_1^3} + \frac{3\mu}{u_2^3} + \frac{3}{u_1^3 u_2^3} \sqrt{\Delta} \right),
 \end{aligned}
 \tag{2.4}$$

where

$$\Delta = (\mu u_1^3 + (1 - \mu) u_2^3)^2 - \mu(1 - \mu) u_1 u_2 (-u_1^4 - u_2^4 + 2u_1^2 + 2u_2^2 + 2u_1^2 u_2^2 - 1).$$

When we restrict to the planar problem ($x_3 = 0$) the Hamiltonian becomes

$$(2.5) \quad H = \frac{1}{2}(y_1^2 + y_2^2) + x_2y_1 - x_1y_2 + \left(\frac{1 - \lambda_2}{2}\right)x_1^2 + \left(\frac{1 - \lambda_1}{2}\right)x_2^2 - \frac{1}{(x_1^2 + x_2^2)^{1/2}} + \frac{c_3}{(x_1^2 + x_2^2)^{3/2}},$$

where the constant terms $\frac{(1-\mu)c_1}{u_1^3}$ and $\frac{\mu c_2}{u_2^3}$ were dropped, as they do not appear in the Hamiltonian equations. We note that in the planar problem the oblateness of the primary and the secondary plays no role.

We denote by \mathbf{M}_h the 3-dimensional energy manifold

$$(2.6) \quad \mathbf{M}_h = \{H = h\}.$$

Remark 2.1. An example of a system that can be modeled by the Hill four-body problem is the Sun-Jupiter-Hektor-Skamandrios system [BGGC⁺20]. Hektor is a Jupiter Trojan, which is approximately located at Lagrangian point L_4 of the Sun-Jupiter system, thus forming an approximate triangular relative equilibrium configuration with Sun and Jupiter. Hektor is the biggest Jupiter Trojan and has one of the largest values of the oblateness coefficients among the objects of its size in the Solar system. Hektor's moonlet, Skamandrios, can be viewed as the fourth, infinitesimal body. In this case, the constants that appear in (2.3) are $c_3 = -1.327161 \times 10^{-7}$, $\mu = 0.0009533386$, $u_1 = 1 - 5.94154 \times 10^{-11}$, $u_2 = 1 - 1.99318 \times 10^{-12}$, $\lambda_1 = 0.002144$, and $\lambda_2 = 2.997855$.

2.2. Main result. The main result of the paper is stated below, and the proof is given in Sections 4 and 6.

Theorem 2.2. *For the system (2.5) with oblate tertiary, i.e., $c_3 < 0$, each collision solution is branch regularizable, and each extension of a collision solution is a reflection. The collision manifold is not block regularizable.*

At $c_3 = 0$ the reduced system of equations associated to the collision manifold undergoes a double saddle-node bifurcation. For $c_3 = 0$, the collision manifold is branch and block regularizable.

For the system (2.5) with a prolate tertiary, i.e., $c_3 > 0$, there are no collisions.

The collision manifold and the corresponding reduced system of equations are described in Section 6.

3. BRANCH AND BLOCK REGULARIZATION

We give a brief review of branch and block regularization following [McG81].

For a differential equation

$$(3.1) \quad \dot{\mathbf{x}} = F(\mathbf{x})$$

with F a real analytic vector field on some open set $U \subseteq \mathbb{R}^n$, and $\dot{\cdot} = \frac{d}{dt}$. The standard existence and uniqueness theorem for ODE's gives for each

initial condition $\mathbf{x}(0) \in U$ a unique, real analytic solution $\mathbf{x}(t)$ defined on a maximal interval (t^-, t^+) with $-\infty \leq t^- < 0 < t^+ \leq +\infty$. Solutions for which $-\infty < t^-$ or $t^+ < +\infty$ are said to have a singularity at $t^* = t^-$ or $t^* = t^+$, respectively.

We briefly describe the concept of branch regularization.

If $\mathbf{x}_1(t)$ and $\mathbf{x}_2(t)$ are solutions of (3.1), with \mathbf{x}_1 ending in a singularity at time t^* and \mathbf{x}_2 beginning in a singularity at t^* , and there exists a multivalued analytic complex function having a branch at t^* and extending both \mathbf{x}_1 and \mathbf{x}_2 when we regard the time t as complex, then $\mathbf{x}_1, \mathbf{x}_2$ are said to be branch extensions of one another at t^* .

A solution $\mathbf{x}(t)$ of equation(3.1) with a singularity at t^* is said to be branch regularizable at t^* if it has a unique branch extension at t^* . The extension is called a ‘reflection’ if the velocity vector reverses direction at collision, and is called a ‘transmission’ if the direction of the velocity vector is preserved at collision. See Fig. 2 (a) and (b).

The equation (3.1) is said to be branch regularizable if every solution is branch regularizable at every singularity.

Now, consider the motion of a single particle in a potential field given by

$$(3.2) \quad U(\mathbf{x}) = |\mathbf{x}|^{-\alpha} \text{ with } \mathbf{x} \in \mathbb{R}^2.$$

The equation of motion is given by the second order equation

$$\ddot{\mathbf{x}} = \nabla U(\mathbf{x}),$$

or equivalently, by the first order system

$$\begin{cases} \dot{\mathbf{x}} = \mathbf{y}, \\ \dot{\mathbf{y}} = -\alpha|\mathbf{x}|^{-\alpha-2}\mathbf{x}. \end{cases}$$

Let $\beta = \frac{\alpha}{2}$ and $\gamma = \frac{1}{1+\beta} = \frac{2}{2+\alpha}$.

We recall the following result from [McG81]:

Theorem 3.1. *A collision solution for the potential (3.2) is branch regularizable if and only if $\gamma = \frac{p}{q}$ with $p < q$ positive integers, $\gcd(p, q) = 1$, and q odd.*

Moreover, if p is even the extension solution is a ‘reflection’, and when p is odd the extension solution is a ‘transmission’.

In [SSM00] this result has been extended for quasi-homogeneous potentials of the form

$$(3.3) \quad U(\mathbf{x}) = \gamma_1|\mathbf{x}|^{-\alpha_1} + \gamma_2|\mathbf{x}|^{-\alpha_2} \text{ with } \mathbf{x} \in \mathbb{R}^2,$$

where $\gamma_1, \gamma_2 > 0, \alpha_2 > \alpha_1 > 0$.

Theorem 3.2. *A collision solution for the potential (3.3) is branch regularizable if and only if both*

$$\frac{2}{2 + \max(\alpha_1, \alpha_2)}, \text{ and } \frac{\min(\alpha_1, \alpha_2)}{2 + \max(\alpha_1, \alpha_2)}$$

are of the form $\frac{p}{q}$ with $p < q$ positive integers, $\gcd(p, q) = 1$, and q odd.

We now describe the concept of block regularization. Denote by $\phi^t = \phi(\cdot, t)$ the flow of (3.1).

A compact invariant set $\mathbf{N} \subseteq U$ is called isolated if there exists an open set $V \subseteq U$ – referred to as an isolating neighborhood – such that $\mathbf{N} \subset V$ is the maximal invariant subset of V .

Let $\mathbf{B} \subseteq U$ be a compact set with non-empty interior, and assume that the boundary $\mathbf{b} = \partial\mathbf{B}$ of \mathbf{B} is a smooth submanifold. Define

$$\begin{aligned}\mathbf{b}^+ &= \{\mathbf{x} \in \mathbf{b} \mid \phi(\mathbf{x}, (-\varepsilon, 0)) \cap \mathbf{B} = \emptyset, \text{ for some } \varepsilon > 0\}, \\ \mathbf{b}^- &= \{\mathbf{x} \in \mathbf{b} \mid \phi(\mathbf{x}, (0, \varepsilon)) \cap \mathbf{B} = \emptyset, \text{ for some } \varepsilon > 0\}, \\ \mathbf{t} &= \{\mathbf{x} \in \mathbf{b} \mid \dot{\phi}(\mathbf{x}, 0) \text{ is tangent to } \mathbf{b}\}.\end{aligned}$$

The set \mathbf{B} is called an isolating block if $\mathbf{b}^+ \cap \mathbf{b}^- = \mathbf{t}$.

If \mathbf{N} is an isolated invariant set, we say that \mathbf{B} isolates \mathbf{N} if the interior set $\text{Int}(\mathbf{B})$ of \mathbf{B} is an isolating neighborhood for \mathbf{N} . For every isolated invariant set \mathbf{N} there exists an isolating block which isolates \mathbf{N} . If \mathbf{B} is an isolating block, then there exists an isolated invariant set \mathbf{N} (possibly empty) which is isolated by \mathbf{B} . See [CE71].

The asymptotic sets to \mathbf{N} are defined by

$$\begin{aligned}\mathbf{a}^+ &= \{\mathbf{x} \in \mathbf{b}^+ \mid \phi(\mathbf{x}, (0, +\infty)) \subset \mathbf{B}\} \\ \mathbf{a}^- &= \{\mathbf{x} \in \mathbf{b}^- \mid \phi(\mathbf{x}, (-\infty, 0)) \subset \mathbf{B}\}\end{aligned}$$

The map across the block is defined as

$$\begin{aligned}\Phi : \mathbf{b}^+ \setminus \mathbf{a}^+ &\rightarrow \mathbf{b}^- \setminus \mathbf{a}^-, \\ \Phi(\mathbf{x}) &= \phi(\mathbf{x}, T(\mathbf{x})),\end{aligned}$$

where $T(\mathbf{x}) = \inf\{t > 0 \mid \phi(\mathbf{x}, t) \notin \mathbf{B}\}$ is the time spent inside the block.

If \mathbf{B} is an isolating block, then the application Φ is a diffeomorphism. See [CE71].

An isolating block \mathbf{B} is said to be trivializable if the map Φ extends uniquely to a diffeomorphism from \mathbf{b}^+ to \mathbf{b}^- .

The theory of isolating blocks can be applied to singularities by essentially replacing the role of an isolated invariant set \mathbf{N} as above with the set of singularities, as we shall see below.

In Section 4 we will see that, going through regularized coordinates and time rescaling, the set of singularities for (2.3), which consists of the origin, gets transformed into an invariant set, which is in fact a manifold (referred to as a collision manifold).

Let $F(\mathbf{x})$ be a vector field defined on $U \setminus \mathbf{N}$, where \mathbf{N} is a compact set representing the singularities of the vector field. Let $\mathbf{B} \subseteq U$ be compact set with non-empty interior, such that $\mathbf{b} = \partial\mathbf{B}$ is a smooth submanifold, and with $\mathbf{b} \cap \mathbf{N} = \emptyset$. Define the subsets $\mathbf{b}^+, \mathbf{b}^- \subset \mathbf{b}$ in the same way as above. Under these conditions, the definition of an isolating block is the same as before.

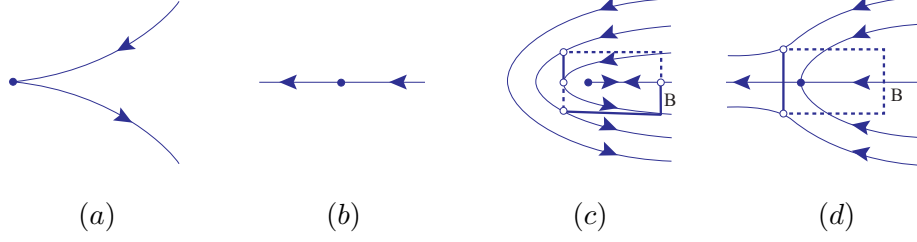


FIGURE 2. Different types of singularities: (a) branch regularizable – reflection, (b) branch regularizable – transmission, (c) block regularizable – the sets a^+ , a^- associated to the block B are marked by dotted and solid lines, respectively, and the set t is marked by empty circles, (d) not block regularizable – same convention as in (c).

The orbit through a point \mathbf{x} is defined by

$$O(\mathbf{x}) = \{ \phi(\mathbf{x}, t) \mid \phi(\mathbf{x}, t) \text{ is defined} \}.$$

That is, there are no invariant sets in \mathbf{B} .

An isolating block \mathbf{B} is said to isolate the singularity set \mathbf{N} if $\mathbf{N} \subset \text{Int}(\mathbf{B})$ and if $O(\mathbf{x}) \not\subset \mathbf{B}$ for all $\mathbf{x} \in \mathbf{B} \setminus \mathbf{N}$.

The asymptotic sets to \mathbf{N} are defined by

$$\mathbf{a}^+ = \{ \mathbf{x} \in \mathbf{b}^+ \mid \phi(\mathbf{x}, t) \in \mathbf{B} \text{ for all } t \geq 0 \text{ for which } \phi(\mathbf{x}, t) \text{ is defined} \}$$

$$\mathbf{a}^- = \{ \mathbf{x} \in \mathbf{b}^- \mid \phi(\mathbf{x}, t) \in \mathbf{B} \text{ for all } t \leq 0 \text{ for which } \phi(\mathbf{x}, t) \text{ is defined} \}.$$

We define the map across the block $\Phi : \mathbf{b}^+ \setminus \mathbf{a}^+ \rightarrow \mathbf{b}^- \setminus \mathbf{a}^-$ as before.

The singularity set \mathbf{N} is said to be block regularizable if there exists a trivialisable block \mathbf{B} which isolates \mathbf{N} . See Fig. 2 (c) and (d).

Regarding block regularization we recall the following result from [McG81]:

Theorem 3.3. *A collision set for the potential (3.2) is block regularizable if and only if $\beta = 1 - \frac{1}{n}$ for n positive integer.*

4. MCGEHEE TRANSFORMATION

We rewrite the Hamiltonian (2.5) in a simpler form

$$(4.1) \quad H = \frac{1}{2}(y_1^2 + y_2^2) + x_2 y_1 - x_1 y_2 + A x_1^2 + B x_2^2 - \frac{1}{(x_1^2 + x_2^2)^{\nu/2}} - \frac{c}{(x_1^2 + x_2^2)^{\alpha/2}},$$

where $\dot{} = \frac{d}{dt}$, and $1 \leq \nu < \alpha$. The corresponding potential is quasi-homogeneous.

In the case of the potential (2.5), we have

$$(4.2) \quad \nu = 1, \quad \alpha = 3, \quad A = \frac{1 - \lambda_2}{2}, \quad B = \frac{1 - \lambda_1}{2}, \quad \lambda_1, \lambda_2 > 0, \quad c = -c_3.$$

We identify $x, y \in \mathbb{R}^2$ with the complex numbers $x_1 + ix_2, y_1 + iy_2$, respectively. The corresponding Hamilton equations are

$$(4.3) \quad \begin{aligned} \dot{x} &= \frac{\partial H}{\partial y} = y - ix, \\ \dot{y} &= -\frac{\partial H}{\partial x} = -\frac{\nu x}{|x|^{\nu+2}} - \frac{\alpha c x}{|x|^{\alpha+2}} - iy - Tx, \end{aligned}$$

where T is the real-linear transformation given by $T(x_1 + ix_2) = 2Ax_1 + 2Bx_2i$, and $|x| = (x_1^2 + x_2^2)^{1/2}$.

We perform a coordinate change to new real coordinates (r, θ, v, w) , with $r > 0$ and $\theta \in \mathbb{T}^1$, defined as follows

$$(4.4) \quad \begin{aligned} x &= r^\gamma e^{i\theta}, \\ y &= r^{-\gamma\beta} (v + iw) e^{i\theta}, \end{aligned}$$

where

$$\beta = \frac{\alpha}{2}, \quad \text{and} \quad \gamma = \frac{1}{\beta + 1} = \frac{2}{\alpha + 2}.$$

Writing (4.4) in terms of components we have

$$(4.5) \quad \begin{aligned} x_1 &= r^\gamma \cos \theta, \\ x_2 &= r^\gamma \sin \theta, \\ y_1 &= r^{-\gamma\beta} (v \cos \theta - w \sin \theta), \\ y_2 &= r^{-\gamma\beta} (v \sin \theta + w \cos \theta). \end{aligned}$$

The new coordinates (r, θ, v, w) in terms of the old coordinates (x_1, x_2, y_1, y_2) are given by

$$(4.6) \quad \begin{aligned} r &= |x|^{\frac{1}{\gamma}}, \\ \theta &= \arg(x), \\ v &= r^{\gamma\beta} (y_1 \cos \theta + y_2 \sin \theta), \\ w &= r^{\gamma\beta} (-y_1 \sin \theta + y_2 \cos \theta). \end{aligned}$$

The new coordinates are known as the McGehee coordinates [McG81]. We rewrite the Hamiltonian equations (4.3) in the new coordinates and equate

the real and imaginary parts on the two sides. From

$$\begin{aligned}
\dot{x} &= \left[\gamma r^{\gamma-1} \dot{r} + i r^\gamma \dot{\theta} \right] e^{i\theta}, \\
\frac{\partial H}{\partial y} &= \left[r^{-\beta\gamma} (v + iw) - i r^\gamma \right] e^{i\theta}, \\
\dot{y} &= \left[-\beta\gamma r^{-\beta\gamma-1} \dot{r} (v + iw) + r^{-\beta\gamma} (\dot{v} + i\dot{w}) + r^{-\beta\gamma} (v + iw) i \dot{\theta} \right] e^{i\theta} \\
&= \left[-\beta r^{-\beta\gamma-1} v (v + iw) + r^{-\beta\gamma} (\dot{v} + i\dot{w}) + r^{-\beta\gamma} (v + iw) i (r^{-1} w - 1) \right] e^{i\theta}, \\
-\frac{\partial H}{\partial x} &= \left[-\frac{\nu r^\gamma}{r^{\gamma(\nu+2)}} - \frac{\alpha c r^\gamma}{r^{\gamma(\alpha+2)}} - i \frac{v + iw}{r^{\gamma\beta}} \right] e^{i\theta} - 2Ar^\gamma \cos \theta - i2Br^\gamma \sin \theta \\
&= \left[-\nu r^{\gamma(-1-\nu)} - \alpha c r^{\gamma(-1-\alpha)} - i(v + iw)r^{-\gamma\beta} \right. \\
&\quad \left. + 2r^\gamma (-A \cos^2 \theta - B \sin^2 \theta) + i2r^\gamma (A - B) \sin \theta \cos \theta \right] e^{i\theta}
\end{aligned}$$

we obtain

$$\begin{aligned}
\dot{r} &= (\beta + 1)v, \\
\dot{\theta} &= r^{-1}w - 1, \\
(4.7) \quad \dot{v} &= \frac{\beta v^2 + w^2 - \alpha c}{r} - \frac{\nu}{r^{\gamma(\nu+2)-1}} - 2Ar \cos^2 \theta - 2Br \sin^2 \theta, \\
\dot{w} &= \frac{(\beta - 1)vw}{r} + 2(A - B)r \sin \theta \cos \theta.
\end{aligned}$$

In the above, after equating $\dot{x} = \frac{\partial H}{\partial y}$ we obtain $\dot{r} = (\beta+1)v$ and $\dot{\theta} = r^{-1}w - 1$, which we substitute in the equation for \dot{y} . We also use that $\frac{1-\gamma}{\gamma} = \beta$, $-\gamma\beta = \gamma - 1$, and $\alpha = 2\beta$. The fact that T is real-linear transformation but not-complex linear is taken into account when factoring out $e^{i\theta}$ in the equation for $-\frac{\partial H}{\partial x}$ by expressing $Tx = (Tx e^{-i\theta})e^{i\theta}$.

The equations (4.7) have a singularity at $r = 0$. We remove the singularity by introducing a new time parameter τ given by

$$(4.8) \quad dt = r d\tau.$$

The equations (4.7) expressed in terms of the new time τ become

$$\begin{aligned}
r' &= (\beta + 1)vr, \\
\theta' &= w - r, \\
(4.9) \quad v' &= (\beta v^2 + w^2 - \alpha c) - \nu r^{2-\gamma(\nu+2)} - 2Ar^2 \cos^2 \theta - 2Br^2 \sin^2 \theta, \\
w' &= (\beta - 1)vw + 2(A - B)r^2 \sin \theta \cos \theta,
\end{aligned}$$

where $' = \frac{d}{d\tau}$. Since $\nu < \alpha$, we have that $2 - \gamma(\nu+2) > 0$. Thus, the obtained differential equations have no singularity at $r = 0$; the singularity has been 'removed'. We also note that the terms $\nu r^{2-\gamma(\nu+2)} - 2Ar^2 \cos^2 \theta - 2Br^2 \sin^2 \theta$ and $2(A - B)r^2 \sin \theta \cos \theta$ tend to 0 as $r \rightarrow 0$, so they can be neglected for r sufficiently small.

The energy condition $H = h$ in the new coordinates, when we use (4.5), becomes

$$(4.10) \quad \begin{aligned} & \frac{1}{2}r^{-2\gamma\beta}(v^2 + w^2) \\ & + r^{\gamma(1-\beta)} \sin \theta (v \cos \theta - w \sin \theta) - r^{\gamma(1-\beta)} \cos \theta (w \cos \theta + v \sin \theta) \\ & + Ar^{2\gamma} \cos^2 \theta + Br^{2\gamma} \sin^2 \theta - r^{-\gamma\nu} - cr^{-\gamma\alpha} = h, \end{aligned}$$

which, after multiplying both sides by $r^{2\gamma\beta} = r^{2-2\gamma}$ yields

$$(4.11) \quad \frac{v^2 + w^2 - 2c}{2} - rw + r^2(A \cos^2 \theta + B \sin^2 \theta) - r^{2-\gamma(\nu+2)} = r^{2-2\gamma} h.$$

We define the *energy manifold* \mathbf{M}_h as the set of points (r, θ, v, w) satisfying (4.11). When $r = 0$ the energy condition (4.11) reduces to

$$(4.12) \quad v^2 + w^2 - 2c = 0.$$

Remark 4.1. In the case of the potential (3.2), one obtains a system of 4-equations similar to (4.9):

$$(4.13) \quad \begin{aligned} r' &= (\beta + 1)vr, \\ \theta' &= w, \\ v' &= \beta(v^2 - 2) + w^2, \\ w' &= (\beta - 1)vw, \end{aligned}$$

This system is partially decoupled – the first two equations are determined by the last two equations. Also, the energy manifold \mathbf{M}_h projects onto $\{v^2 + w^2 < 1\}$ when $h < 0$, onto $\{v^2 + w^2 > 1\}$ when $h > 0$, and onto $\{v^2 + w^2 = 1\}$ when $h = 0$. See[McG81].

In the case of our system (4.9) the second equation has an extra term owed to the Coriolis effect in (2.3), the third equation has extra terms owed to oblateness and to the effects of the primary and secondary, and the fourth equation has an extra term owed to the effect of the primary and secondary.

Also, the system (4.9) is fully coupled, and there is no obvious relation between the regions bounded by $v^2 + w^2 = 2c$ in the (v, w) -plane and the energy h .

Writing the energy condition (4.11) as

$$\begin{aligned} \frac{v^2 + w^2 - 2c}{2} &= r^{2-2\gamma} h + rw - r^2(A \cos^2 \theta + B \sin^2 \theta) + r^{2-\gamma(\nu+2)}, \text{ or} \\ h &= \frac{1}{r^{2-2\gamma}} \left(\frac{v^2 + w^2 - 2c}{2} \right) - \frac{1}{r^{1-2\gamma}} w + r^{2\gamma}(A \cos^2 \theta + B \sin^2 \theta) - \frac{1}{r^{\nu\gamma}}, \end{aligned}$$

we see that for $r \ll 1$ the sign of h is the same as the sign of $v^2 + w^2 - 2c$. Thus, the points in \mathbf{M}_h with $h > 0$ and $r \approx 0$ project onto $\{v^2 + w^2 > 2c\}$ and the points in \mathbf{M}_h with $h < 0$ and $r \approx 0$ project onto $\{v^2 + w^2 < 2c\}$.

5. EQUILIBRIUM POINTS AND HILL REGIONS

A straightforward computations shows that (4.9) has 6 equilibrium points, which in terms of the (r, θ, v, w) -coordinates are given by

$$(5.1) \quad \begin{aligned} \mathcal{E}_\pm &= (0, \theta_0, \pm\sqrt{2c}, 0), \\ \mathcal{E}_1 &= (r_1, 0, 0, r_1), \quad \mathcal{E}_2 = (r_1, \pi, 0, r_1), \\ \mathcal{E}_3 &= (r_2, \pi/2, 0, r_2), \quad \mathcal{E}_4 = (r_2, 3\pi/2, 0, r_2). \end{aligned}$$

for arbitrary $\theta_0 \in \mathbb{T}^1$, r_1 being the solution of

$$(5.2) \quad r^2(1 - 2A) - \nu r^{2-\gamma(\nu+2)} - \alpha c = 0,$$

and r_2 being the solution of

$$(5.3) \quad r^2(1 - 2B) - \nu r^{2-\gamma(\nu+2)} - \alpha c = 0.$$

Note that (5.2) and (5.3) have unique solutions. The equilibrium points $\mathcal{E}_1, \mathcal{E}_2, \mathcal{E}_3, \mathcal{E}_4$ are the same as the x - and y -equilibrium points for the Hill four-body problem in [BGCG⁺20], respectively (referred to as L_1, L_2, L_3, L_4 in [BG16]). The points $\mathcal{E}_1, \mathcal{E}_2$ are of center-saddle type; the points $\mathcal{E}_3, \mathcal{E}_4$ are of center-center type provided that μ is less than some critical value μ_{cr} . On the other hand, \mathcal{E}_\pm form circles of equilibrium points. The eigenvalues at each point of \mathcal{E}_\pm are

$$0, \pm(\beta + 1)\sqrt{2c}, \pm 2\beta\sqrt{2c}, \pm(\beta - 1)\sqrt{2c}.$$

The circle \mathcal{E}_+ has a 4-dimensional unstable manifold and the circle \mathcal{E}_- has a 4-dimensional stable manifold, which necessarily coincide.

The effective potential for the system (4.1) is

$$\Omega(x_1, x_2) = \frac{1}{2} (\lambda_2 x_1^2 + \lambda_1 x_2^2) + \frac{1}{(x_1^2 + x_2^2)^{\nu/2}} + \frac{c}{(x_1^2 + x_2^2)^{\alpha/2}},$$

which, written in McGehee coordinates becomes

$$\Omega(r, \theta) = \frac{1}{2} (\lambda_2 r^{2\gamma} \cos^2(\theta) + \lambda_1 r^{2\gamma} \sin^2(\theta)) + r^{-\nu\gamma} + cr^{-\alpha\gamma}.$$

Then the Hill region for an energy level h , defined as the projection on the energy manifold onto configuration space, represents the region of possible motions, and is given by

$$\{(r, \theta) \mid \Omega(r, \theta) \geq -h\}$$

which, after multiplying both sides by $r^{2-2\gamma}$ becomes

$$\left\{ (r, \theta) \mid \frac{1}{2} (\lambda_2 r^2 \cos^2(\theta) + \lambda_1 r^2 \sin^2(\theta)) + r^{2-\gamma(\nu+2)} + c + hr^{2-2\gamma} \geq 0 \right\}$$

The Hill region for the energy levels below, at, and above that of the equilibrium points $\mathcal{E}_1, \mathcal{E}_2$, is shown in Fig. 3.

The system (4.9) allows the study of the dynamics both near and far from collisions. In particular, it can be used to compute families of orbits that start far from collision and tend asymptotically to collision. For example, we

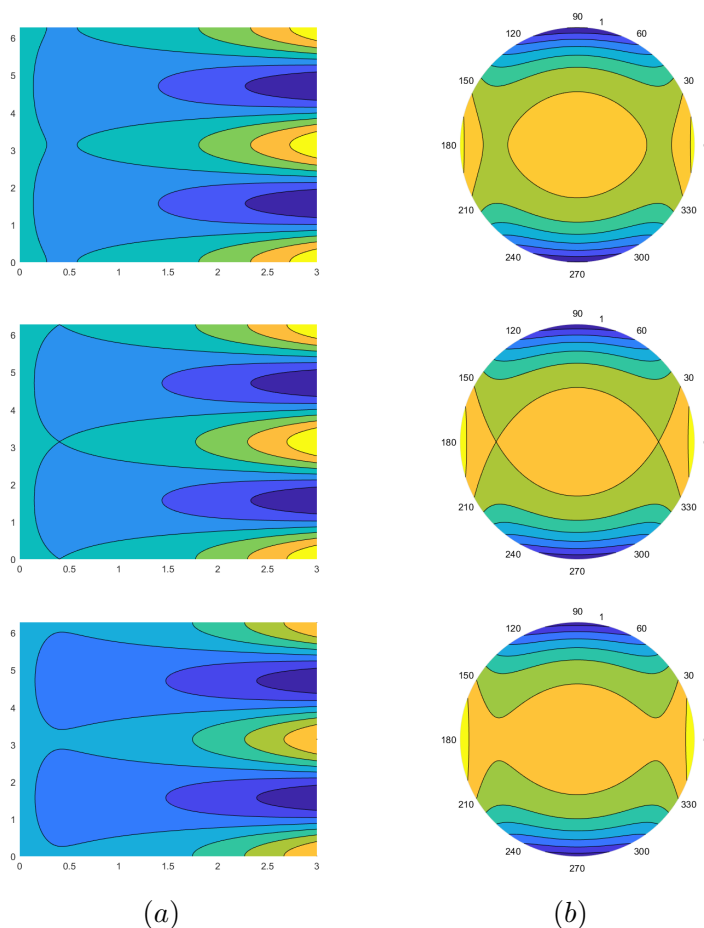


FIGURE 3. Hill region for energy levels below, at, and above that of $\mathcal{E}_1, \mathcal{E}_2$ in McGehee coordinates: (a) in (r, θ) -coordinates, (b) in (x, y) -coordinates.

can compute the so called ‘long’ and ‘short’ period families of periodic orbits near $\mathcal{E}_3, \mathcal{E}_4$, which were studied in [BG16]. Such families of periodic orbits were originally considered in [DJP⁺67] in the context of the planar circular restricted three-body problem, where they emanate from the center-center equilibrium points L_3 and L_4 . Such equilibrium points do not exist in the Hill three-body problem, but they appear in the Hill four-body problem, as noted in [BGG15]. The long period family of orbits undergoes a bifurcation with the short period family, and the short family approaches a collision with the tertiary as the energy h tends to $+\infty$. An orbit from the short period family, computed in both Cartesian and McGehee coordinates, is shown in Fig. 4.

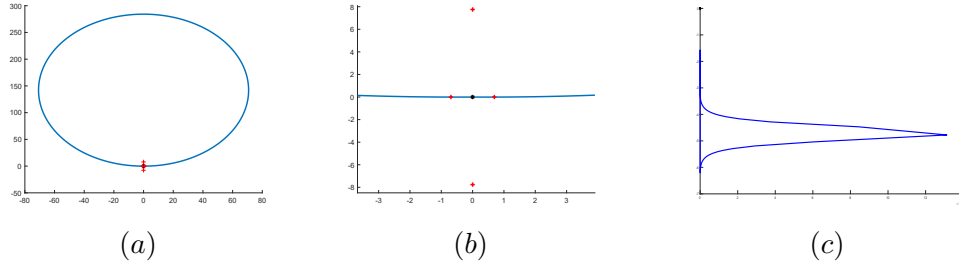


FIGURE 4. Short period orbit near collision: (a) in (x, y) -Cartesian coordinates, (b) in (x, y) -Cartesian coordinates – magnification near the tertiary (marked by $*$) and the $\mathcal{E}_1, \mathcal{E}_2, \mathcal{E}_3, \mathcal{E}_4$ equilibrium points (marked by $+$), (c) in (r, θ) -coordinates.

6. COLLISION MANIFOLD

From (4.12), the intersection between the energy manifold \mathbf{M}_h and the 3-dimensional hyperplane

$$\mathbf{Z} = \{r = 0\}$$

is a 2-dimensional manifold corresponding to collisions

$$(6.1) \quad \mathbf{N} = \{H = h\} \cap \{r = 0\}.$$

It is referred to as the *collision manifold*. Thus, from (4.12) we obtain that

$$(6.2) \quad \mathbf{N} = \{(r, \theta, v, w) \mid r = 0, \theta \in \mathbb{T}^1, v^2 + w^2 = 2c\},$$

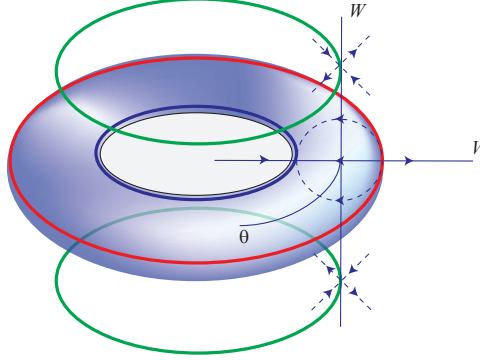
so the collision manifold is a *2-dimensional torus* provided $c > 0$. Note that this torus is independent of the energy level h , and is the boundary of each energy manifold \mathbf{M}_h .

The collision manifold is an isolated invariant set for the flow of (4.9). If a trajectory approaches the singularity, i.e., $r \rightarrow 0$ as $t \rightarrow \pm t^*$, then in the (r, θ, v, w) coordinates the trajectory approaches the collision manifold \mathbf{N} as $\tau(t) \rightarrow \mp \infty$. The argument is the same as in [McG81].

Since $r' = 0$ when $r = 0$, it follows that the set \mathbf{Z} is invariant under the solutions of the system (4.9). Thus, we can consider the restriction of (4.9) to \mathbf{Z} , which is given by

$$(6.3) \quad \begin{aligned} \theta' &= w, \\ v' &= \beta v^2 + w^2 - \alpha c, \\ w' &= (\beta - 1)vw. \end{aligned}$$

The dynamics on \mathbf{Z} is the skew product between the dynamics in the variables (v, w) and the dynamics in θ . See Fig. 5. The solution of the equation in θ is determined by the solutions of the (v, w) -subsystem, which is independent of θ . We refer to the (v, w) -subsystem of (6.3) as the *reduced system associated to the collision manifold*.

FIGURE 5. The dynamics on \mathbf{N} and \mathbf{Z}

Define

$$(6.4) \quad K = |w|^\alpha |v^2 + w^2 - 2c|^{1-\beta}.$$

We claim that K is an integral of motion for the (v, w) -subsystem of (6.3). Indeed, using (6.3) we obtain

$$\begin{aligned} K' &= \alpha |w|^{\alpha-1} w' |v^2 + w^2 - 2c|^{1-\beta} + |w|^\alpha |v^2 + w^2 - 2c|^{-\beta} (2vv' + 2ww') \\ &= \alpha |w|^{\alpha-1} (\beta - 1) vw |v^2 + w^2 - 2c|^{1-\beta} \\ &\quad + |w|^\alpha |v^2 + w^2 - 2c|^{-\beta} (2v(\beta v^2 + w^2 - \alpha c) + 2w(\beta - 1)vw) \\ &= |w|^{\alpha-1} |v^2 + w^2 - 2c|^{-\beta} (\beta - 1) vw [\alpha(v^2 + w^2 - 2c) \\ &\quad - 2(\beta v^2 + w^2 - \alpha c) - 2(\beta - 1)w^2] \\ &= 0. \end{aligned}$$

By (6.2), the collision manifold \mathbf{N} intersects the (v, w) -plane along the 0-level set of the integral K .

We now describe the geometry of the (v, w) -subsystem. The equilibrium points are $S_\pm = (\pm\sqrt{2c}, 0)$ and $Q_\pm = (0, \pm\sqrt{\alpha c})$. The circle

$$\mathbf{C} = \{v^2 + w^2 = 2c\}$$

is invariant under the flow of the subsystem, and passes through the points S_\pm . Thus, S_\pm correspond to points on the collision manifold \mathbf{N} , while Q_\pm do not.

The circle \mathbf{C} in the (v, w) -plane corresponds to the collision manifold \mathbf{N} , while the other orbits of the (v, w) -subsystem represent projections of orbits on various energy levels onto the (v, w) -plane.

The eigenvalues of the linearized system at Q_\pm are

$$\pm\sqrt{2(\beta - 1)\alpha c},$$

and since one is positive and the other is negative, both points are saddle points. The eigenvalues of the linearized system at S_{\pm} are

$$\pm 2\beta\sqrt{2c}, \quad \pm(\beta - 1)\sqrt{2c}.$$

Both eigenvalues at S_+ are positive hence this is a source. Both eigenvalues at S_- are negative hence this is a sink. The line $w = 0$ is also invariant under the flow, where $v' < 0$ for $|v| < \sqrt{2c}$ and $v' > 0$ for $|v| > \sqrt{2c}$. The phase portrait is shown in Fig. 6.

Each point Q_{\pm} has 1-dimensional stable and unstable manifolds in the (v, w) -plane; these manifolds are asymptotic to S_{\pm} . In the full phase space, the points Q_{\pm} lie on circular orbits \mathcal{C}_{\pm} given by

$$r = 0, \quad \theta = \theta_0 \pm t\sqrt{\alpha c}, \quad v = 0, \quad w = \pm\sqrt{\alpha c}, \quad \text{for } t \in \mathbb{R},$$

of energy $+\infty$. Each circle \mathcal{C}_{\pm} has 2-dimensional stable and unstable manifolds in \mathbf{Z} .

The points S_{\pm} lie on the circles of equilibria \mathcal{E}_{\pm} contained in \mathbf{N} . The circle \mathcal{E}_+ has a 2-dimensional unstable manifold in \mathbf{N} , while the circle \mathcal{E}_- has a 2-dimensional stable manifold in \mathbf{N} ; the stable and unstable manifolds coincide. In \mathbf{Z} the circle \mathcal{E}_+ has a 3-dimensional unstable manifold, and the circle \mathcal{E}_- has a 3-dimensional stable manifold; these manifolds coincide as well.

We summarize the type of orbits that appear near collision:

Orbits beginning and ending in collision: These orbits form an open set in the phase space, representing the branch of the unstable manifold of \mathcal{E}_+ that coincides with a branch of stable manifold of \mathcal{E}_- . Such orbits correspond to initial conditions whose projection onto the (v, w) -plane is in $\{(v, w) \mid v^2 + w^2 < 2c\}$.

Orbits that only begin or only end in collision: These orbits form open sets in the phase space, representing the branches of the unstable manifold of \mathcal{E}_+ and of the stable manifold of \mathcal{E}_- , respectively, whose projection onto the (v, w) -plane is in $\{(v, w) \mid v^2 + w^2 > 2c\}$.

Asymptotic orbits than begin or end in collision: These orbits represent branches of the stable and unstable manifolds of the hyperbolic invariant circles \mathcal{C}_{\pm} .

Swing-by orbits: These are orbits coming from afar, passing near the hyperbolic invariant circles \mathcal{C}_{\pm} , and then moving away.

Recall that for the system 2.5 we have $\nu = 1$, $\alpha = 3$, $\beta = \frac{3}{2}$, and $\gamma = \frac{2}{5}$. By Theorem 3.2 it follows that each collision solution is branch regularizable. Since $p = 2$ is even, each extension solution is a ‘reflection’.

By examining Fig. 6 we observe that the collision manifold \mathbf{N} is not an isolated invariant set, and therefore it is not block regularizable. This agrees with the case of the potential (3.2), where for $\beta \geq 1$ the collision manifold \mathbf{N} is not an isolated set.

As $c \rightarrow 0$, the two saddles, the source, and the sink coalesce through a double saddle-node bifurcation. See Fig. 7.

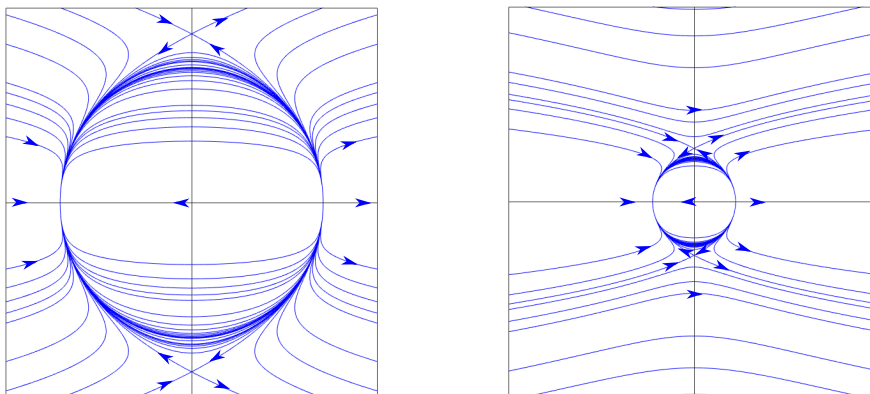


FIGURE 6. Left: $c = 1$. Right: $c = 0.1$.

For $c = 0$ the collision manifold is reduced to a point, and it is both branch and block regularizable.

We now discuss the case when $c < 0$. This describes a situation when the tertiary is a prolate body. In this case the set of (v, w) with $v^2 + w^2 = 2c$ is the empty set. Thus the collision set \mathbf{N} is empty. Then the (v, w) -subsystem

$$(6.5) \quad \begin{aligned} v' &= \beta v^2 + w^2 - \alpha c, \\ w' &= (\beta - 1)vw, \end{aligned}$$

has the property that $v' > 0$. The phase portrait is shown in Fig. 7. In this case there are no collisions.

The physical interpretation is the following. Denoting $c = -\tilde{c}$ where $\tilde{c} > 0$, the Hamiltonian (2.5) becomes

$$(6.6) \quad \begin{aligned} H &= \frac{1}{2}(y_1^2 + y_2^2) + x_2 y_1 - x_1 y_2 + A x_1^2 + B x_2^2 \\ &\quad - \frac{1}{|x|^{\nu/2}} + \frac{\tilde{c}}{|x|^{\alpha/2}}. \end{aligned}$$

The term $-\frac{1}{|x|^{\nu/2}}$ in the potential corresponds to an attractive force, and the term $\frac{\tilde{c}}{|x|^{\alpha/2}}$ corresponds to a repulsive force. When the particle approaches the tertiary, since $1 \leq \nu < \alpha$ the repulsive force becomes dominating, preventing collisions between the particle and the tertiary to occur. This situation is also described in [Saa74].

Remark 6.1. One can consider a simple model that takes into account the size of the asteroid. Since $\nu = 1$, $\alpha = 3$, $\beta = \frac{3}{2}$, and $\gamma = \frac{2}{5}$, the powers of r that appear in (4.9) are

$$r^{2-\gamma(1+\nu)} = r^{4/5} \gg r \gg r^2.$$

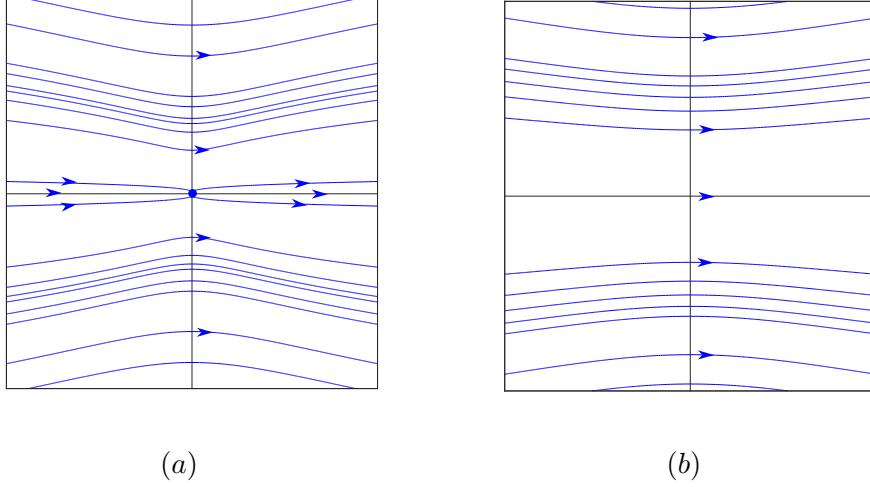


FIGURE 7. Phase portrait of the (v, w) -subsystem: (a) $c = 0$, (b) $c = -1$.

We can neglect the powers r^k of r with $k > 4/5$. Then collisions correspond to setting $r = R_3$, the average radius of the tertiary; in the case of Hektor, in the normalized units $R_3 = 1.18716 \times 10^{-7}$. Then (4.9) yields

$$(6.7) \quad \begin{aligned} \theta' &= w, \\ v' &= (\beta v^2 + w^2 - \alpha c) - \nu R_3^{2-\gamma(\nu+2)}, \\ w' &= (\beta - 1)vw. \end{aligned}$$

This system is essentially the same as the system (6.3) with the term $-\alpha c$ replaced with the term $-\alpha c - \nu R_3^{2-\gamma(\nu+2)}$. Then the analysis of collisions is similar to the one above. Another possibility could be to neglect the powers r^k of r with $k > 1$. Of course, it is possible to consider more sophisticated models that take into account the dumbbell shape of Hektor or more general asteroid shapes, in which case the gravitational potential (2.1) needs to be modeled differently, e.g., [LGZ21].

Remark 6.2. There are several moons in the Solar System that are considered to be approximately prolate spheroids in shape, for example, Uranus' moons Cordelia, Cressida, Desdemona, Juliet, Ophelia, and Rosalind.

Remark 6.3. The (v, w) -subsystem of (6.3) is undergoing another bifurcation at $\alpha = 2$ when $c > 0$ is held fixed. When $\alpha = 2$ the points Q_{\pm} lie on the collision manifold. When $\alpha < 2$, the points Q_{\pm} become centers, and the points S_{\pm} become saddles. The phase portrait is as in Fig. 8.

Remark 6.4. In the case when $c = 0$, the term $-\frac{c}{|x|^{\alpha}}$ in (4.1) vanishes. Then one can perform the coordinate change (4.4) with $\gamma = \frac{2}{2+\nu}$ and $\beta = \frac{\nu}{2}$,

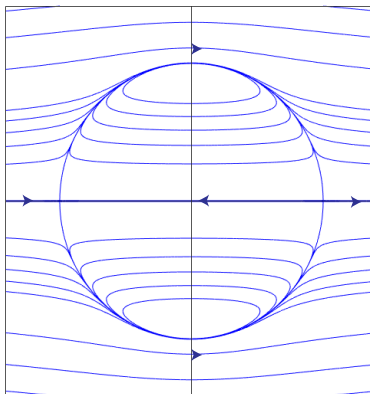


FIGURE 8. Phase portrait of the (v, w) -subsystem for $\alpha < 2$ and $c > 0$.

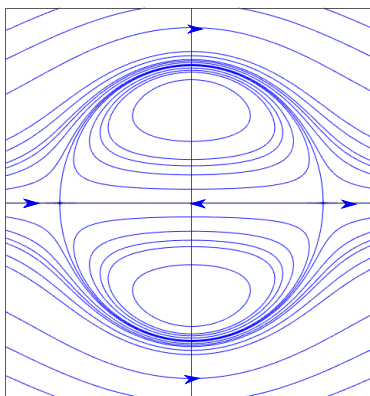


FIGURE 9. Phase portrait of the (v, w) -subsystem for $c = 0$ with the coordinate change (4.4) with $\gamma = \frac{2}{2+\nu}$ and $\beta = \frac{\nu}{2}$.

as in [McG81]. The resulting collision manifold is a torus which intersects the (v, w) -plane in a circle as in Fig. 9. Note that the phase portrait is qualitatively the same as in Fig. 8. It contains two circles of equilibria located at $v = \pm\sqrt{2}$ and a cylinder of orbits given by $w = 0$ connecting the two circles. The collision set is both branch and block regularizable. It is interesting that this coordinate change leads to a different collision manifold from the one in (6.2), but nevertheless its branch and block regularization properties are the same.

7. CONCLUSIONS

In this paper we provide an explicit McGehee coordinate transformation to regularize collision in the planar Hill four-body problem with oblate bodies. This transformation can be used to understand the behavior of collision and near-collision orbits. In particular, our formulas can be implemented in numerical integrators to compute orbits that pass close to an oblate Jupiter’s trojan asteroid.

We also describe the collision manifold and show that it undergoes a bifurcation as the oblateness coefficient of the asteroid passes through the zero value. We note here that the bifurcation observed for this system is very different from the one described by [McG81] for the potential energy $U(\mathbf{x}) = |\mathbf{x}|^{-\alpha}$ in (3.2), which undergoes a bifurcation when the parameter α passes through the critical value $\alpha_{\text{cr}} = 2$.

It is interesting to note that when the oblateness approaches zero (and hence the gravitational potential becomes Newtonian), the limiting collision manifold that we obtain is not the same as the collision manifold obtained by applying the McGehee coordinate transformation to the Newtonian potential. It would be interesting to see if there is a McGehee-type coordinate transformation for which the limiting collision manifold is the same as in the Newtonian case. Another interesting problem would be to extend these results to the spatial Hill four-body problem with oblate bodies.

ACKNOWLEDGEMENTS

We are grateful to Jaime Burgos-García for useful discussions.

REFERENCES

- [ARBMO21] Martha Alvarez-Ramírez, Esther Barrabés, Mario Medina, and Merce Ollé. Ejection–collision orbits in two degrees of freedom problems in celestial mechanics. *Journal of Nonlinear Science*, 31(4):1–33, 2021.
- [Bel13] Edward Belbruno. On the regularizability of the big bang singularity. *Celestial Mechanics and Dynamical Astronomy*, 115(1):21–34, 2013.
- [BG16] Jaime Burgos-García. Families of periodic orbits in the planar Hill’s four-body problem. *Astrophysics and Space Science*, 361(11):1–21, 2016.
- [BGCG⁺20] Jaime Burgos-García, Alessandra Celletti, Catalin Gales, Marian Gidea, and Wai-Ting Lam. Hill Four-Body Problem with Oblate Bodies: An Application to the Sun–Jupiter–Hektor–Skamandrios System. *Journal of Nonlinear Science*, pages 1–46, 2020.
- [BGG15] Jaime Burgos-García and Marian Gidea. Hill’s approximation in a restricted four-body problem. *Celestial Mechanics and Dynamical Astronomy*, 122(2):117–141, 2015.
- [BP11] Edward Belbruno and Frans Pretorius. A dynamical system’s approach to Schwarzschild null geodesics. *Classical and Quantum Gravity*, 28(19):195007, 2011.
- [BX18] Edward Belbruno and BingKan Xue. Regularization of the big bang singularity with random perturbations. *Classical and Quantum Gravity*, 35(6):065013, 2018.

- [CE71] Charles Conley and Robert Easton. Isolated invariant sets and isolating blocks. *Transactions of the American Mathematical Society*, 158(1):35–61, 1971.
- [Des15] Pascal Descamps. Dumb-bell-shaped equilibrium figures for fiducial contact-binary asteroids and EKBOs. *Icarus*, 245:64 – 79, 2015.
- [Dev81] Robert L Devaney. Singularities in classical mechanical systems. In *Ergodic theory and dynamical systems I*, pages 211–333. Springer, 1981.
- [DJP⁺67] André Deprit, Henrard Jacques, Julian Palmore, JF Price, and DH Sadler. The Trojan manifold in the system Earth–Moon. *Monthly Notices of the Royal Astronomical Society*, 137(3):311–335, 1967.
- [DMS00] Florin Diacu, Vasile Mioc, and Cristina Stoica. Phase-space structure and regularization of Manev-type problems. *Nonlinear Analysis: Theory, Methods & Applications*, 41(7-8):1029–1055, 2000.
- [Eas71] Robert Easton. Regularization of vector fields by surgery. *Journal of Differential Equations*, 10(1):92–99, 1971.
- [ElB09] Mohamed Sami ElBialy. Collective branch regularization of simultaneous binary collisions in the 3D N-body problem. *Journal of mathematical physics*, 50(5):052702, 2009.
- [Fer88] Joaquín Delgado Fernández. Transversal ejection-collision orbits in Hill’s problem for $C \gg 1$. *Celestial mechanics*, 44(3):299–307, 1988.
- [GM14] Pablo Galindo and Marc Mars. McGehee regularization of general SO (3)-invariant potentials and applications to stationary and spherically symmetric spacetimes. *Classical and Quantum Gravity*, 31(24):245008, 2014.
- [LGZ21] Wai-Ting Lam, Marian Gidea, and Fredy R Zypman. Surface gravity of rotating dumbbell shapes. *Astrophysics and Space Science*, 366(3):1–9, 2021.
- [LL88] Ernesto A Lacomba and Jaume Llibre. Transversal ejection-collision orbits for the restricted problem and the Hill’s problem with applications. *Journal of differential equations*, 74(1):69–85, 1988.
- [Lli82] Jaume Llibre. On the restricted three-body problem when the mass parameter is small. *Celestial mechanics*, 28(1):83–105, 1982.
- [McG81] Richard McGehee. Double collisions for a classical particle system with non-gravitational interactions. *Commentarii Mathematici Helvetici*, 56(1):524–557, 1981.
- [MDCR⁺14] F. Marchis, J. Durech, J. Castillo-Rogez, F. Vachier, M. Cuk, J. Berthier, M.H. Wong, P. Kalas, G. Duchene, M.A. Van Dam, et al. The puzzling mutual orbit of the binary Trojan asteroid (624) Hektor. *The Astrophysical journal letters*, 783(2):L37, 2014.
- [ORS18] Mercè Ollé, Òscar Rodríguez, and Jaume Soler. Ejection-collision orbits in the RTBP. *Communications in Nonlinear Science and Numerical Simulation*, 55:298–315, 2018.
- [ORS22] M. Ollé, Ó. Rodríguez, and J. Soler. Study of the ejection/collision orbits in the spatial RTBP using the McGehee regularization. *Communications in Nonlinear Science and Numerical Simulation*, 111:106410, 2022.
- [Pin95] Conxita Pinyol. Ejection-collision orbits with the more massive primary in the planar elliptic restricted three body problem. *Celestial Mechanics and Dynamical Astronomy*, 61(4):315–331, 1995.
- [Saa74] Donald G Saari. Regularization and the artificial Earth satellite problem. *Celestial mechanics*, 9(1):55–72, 1974.
- [SSM00] Gheorghe Stoica, Cristina Stoica, and Vasile Mioc. Branch regularization of quasihomogeneous functions. *Revue Roumaine de Mathematiques Pures et Appliquees*, 45(5):897–906, 2000.

- [XB14] BingKan Xue and Edward Belbruno. Regularization of the big bang singularity with a time varying equation of state $w > 1$. *Classical and Quantum Gravity*, 31(16):165002, 2014.

YESHIVA UNIVERSITY, DEPARTMENT OF MATHEMATICAL SCIENCES, NEW YORK, NY 10016, USA

Email address: `edward.belbruno@yu.edu`

YESHIVA UNIVERSITY, DEPARTMENT OF MATHEMATICAL SCIENCES, NEW YORK, NY 10016, USA

Email address: `Marian.Gidea@yu.edu`

FLORIDA ATLANTIC UNIVERSITY, DEPARTMENT OF MATHEMATICAL SCIENCES, BOCA RATON, FL 33431, USA

Email address: `WaiTing.Lam@yu.edu`